

Certified Quantum Measurement of Majorana Fermions

Abu Ashik Md. Irfan,^{1,*} Karl Mayer,^{2,3,*} Gerardo Ortiz,¹ and Emanuel Knill^{2,4}

¹*Department of Physics, Indiana University, Bloomington, IN 47405-7105, USA*

²*National Institute of Standards and Technology, Boulder, Colorado, USA*

³*Department of Physics, University of Colorado, Boulder, Colorado, USA*

⁴*Center for Theory of Quantum Matter, University of Colorado, Boulder, Colorado, USA*

(Dated: January 2, 2020)

We present a quantum self-testing protocol to certify measurements of fermion parity involving Majorana fermion modes. We show that observing a set of ideal measurement statistics implies anti-commutativity of the implemented Majorana fermion parity operators, a necessary prerequisite for Majorana detection. Our protocol is robust to experimental errors. We obtain lower bounds on the fidelities of the state and measurement operators that are linear in the errors. We propose to analyze experimental outcomes in terms of a contextuality witness W , which satisfies $\langle W \rangle \leq 3$ for any classical probabilistic model of the data. A violation of the inequality witnesses quantum contextuality, and the closeness to the maximum ideal value $\langle W \rangle = 5$ indicates the degree of confidence in the detection of Majorana fermions.

I. INTRODUCTION

Topological qubits offer promising basic units for quantum information processing due to their inherent resilience against decoherence¹. Majorana fermions² are candidates for realizing such topological qubits, and the ability to braid them is the focus of several recent investigations. Theoretically, Majorana fermions emerge from the interplay between the existence of a topologically non-trivial vacuum and a, typically, symmetry-protected physical boundary (or defect). They are realized as zero-energy modes or quasi-particle excitations of certain quantum systems. Recent experimental efforts to detect and control Majorana zero-energy modes in topological superconducting nanowires provide a step towards realizing non-Abelian braiding and, thus, topological computation. Several experimental groups have reported evidence of Majorana zero-energy modes, such as an observation of a zero bias conductance peak or Shapiro steps in superconducting nanowires^{3,4}. The evidence, however, remains indirect and it is unclear what would constitute proof of the existence of Majorana fermions⁵. Moreover, interpretation of what embodies a Majorana excitation, and its physical realization, in a closed particle number-conserving many-body topological superfluid deepens the mystery^{6,7}.

Even if one had strong evidence that a system is in a topological superfluid phase with emerging Majorana fermions, in order to reap the advantages of the topological approach to quantum computing, one must be confident that the measurements performed actually implement ideal quantum operations with high fidelity. This is especially important for proposals where gates are performed by parity measurements and anyonic teleportation, rather than physical braiding⁸. In this paper, we present a protocol to certify quantum measurements of observables and states using only the statistics of measurements outcomes, while making no assumptions about the underlying physics in the experimental apparatus. Our technique represents an extension of what is known

as *self-testing* in quantum information^{9–11}. In particular, we are interested in currently proposed platforms utilizing fermionic parity measurements¹². In this way, and given experimental data, one hopes to argue for the consistency of that data with the existence of Majorana fermions.

In the quantum information literature, self-testing refers to the action of uniquely determining a quantum state, up to a certain notion of equivalence. Unlike tomography, self-testing is based solely on the statistics of measurement outcomes, with minimal assumptions about the measurement operators. These quantum self-testing protocols are more stringent than the well-known Bell tests¹³. While violation of a Bell inequality for a bipartite system establishes that its quantum state is entangled, it cannot certify, for instance, that its quantum state is maximally entangled^{14,15}. Self-testing protocols typically assume that the physical system has a Hilbert space with a natural local tensor product structure. For self-testing a fermionic system, however, we have to relax this assumption. In our scenario, involving 6 Majorana fermion modes and 6 parity operators, a minimal assumption is compatibility of observables sharing no common putative Majorana mode. A successful certification implies that the experimentally measured observables anti-commute exactly the way ideal fermionic parity operators should. We demonstrate that ideal statistics imply *emergence* of an invariant four-dimensional tensor-product subspace (encoding two logical qubits) out of a putative Majorana fermion non-tensor-product state space, and the ideal state is a Bell state up to local unitary equivalence. An observation of the ideal statistics in our protocol would constitute substantive evidence of the existence of Majorana fermions. This is so, since ideal statistics implies anti-commutativity of a Majorana fermion and its parity operator, a definite smoking gun for Majorana fermion detection. Experiments, however, suffer from imperfections, and any practical certification protocol should include the effect of non-ideal quantum measurement devices and procedures. We have obtained

lower bounds on state and operator fidelities, linear in the error, that constitute rigorous statements on robustness of the self-testing protocol for detection of Majorana fermions.

The paper is organized as follows. Preliminary background concepts and strategy for self-testing Majorana fermion parities are discussed in Sec. II. In particular, in Sec. II A, we map Majorana fermion parity operators to two-qubit Pauli operators, and construct maximal sets of compatible measurements, so-called contexts. In Sec. II B, we introduce the notion of quantum self-testing. Section III describes our particular measurement scenario and contains a summary of our main results, which are two theorems, proved later in Sections IV and V. Specifically, we prove *rigidity* of the measurement scenario in Sec. IV, and address the *robustness* to small experimental errors in Sec. V. Finally, in Sec. VI we summarize main findings and analyze our fermion parity certification protocol from the standpoint of a contextuality witness W . We suggest a possible experimental setup and propose to analyze experimental data validating a contextuality inequality involving such W . We also emphasize the generality of our approach and its potential application to other quantum measurements involving phenomena such as braiding. An accessible discussion, addressed to experimentalists, of what an ideal statistics situation means in the context of self-testing fermion parities is presented in Appendix A. Several technical details, important to appreciate the mathematical and physical implications of our results, are included in Appendices B, C, D, and E.

II. BACKGROUND

A. Majorana Fermions

Logical Qubits	Fermion Parities	Physical Qubits
00⟩	+, +, +⟩	↓⟩ ⊗ Φ ₋ ⟩
	- , +, +⟩	↓⟩ ⊗ Φ ₋ ′⟩
01⟩	- , +, -⟩	- ↓⟩ ⊗ Φ ₊ ⟩
	+, +, -⟩	- ↓⟩ ⊗ Φ ₊ ′⟩
10⟩	- , -, +⟩	↑⟩ ⊗ Φ ₋ ′⟩
	+, -, +⟩	- ↑⟩ ⊗ Φ ₋ ⟩
11⟩	+, -, -⟩	- ↑⟩ ⊗ Φ ₊ ′⟩
	- , -, -⟩	↑⟩ ⊗ Φ ₊ ⟩

TABLE I. Mapping between the (logical) 4-dimensional and (physical) 8-dimensional spaces (fermion parity assignments for P_{36} , P_{12} and P_{45} and three qubits representations). For each logical state the upper row corresponds to even parity, while the lower to odd parity. Here, $|\Phi_{\pm}\rangle = \frac{|\uparrow\uparrow\rangle \pm |\downarrow\downarrow\rangle}{\sqrt{2}}$ and $|\Phi'_{\pm}\rangle = \frac{|\uparrow\downarrow\rangle \pm |\downarrow\uparrow\rangle}{\sqrt{2}}$.

Majorana fermion modes are potential blueprint qubits for topological computation. Consider 6 Majorana modes belonging to 6 different quantum wires or vortices. Those modes are defined by Majorana operators γ_j for $j =$

$1, \dots, 6$, which satisfy the Majorana algebra

$$\gamma_j^\dagger = \gamma_j, \text{ and } \{\gamma_j, \gamma_k\} = \gamma_j \gamma_k + \gamma_k \gamma_j = 2\delta_{jk}.$$

The complex \dagger -closed algebra generated is \dagger -isomorphic to the complex 8×8 matrices, so its irreducible representations on a Hilbert space all can be identified with a Jordan-Wigner representation on 3 two-level (qubit) systems. Explicitly, one such representation maps

$$\begin{aligned} \gamma_{2m-1} &= \left(\prod_{\ell=1}^{m-1} \sigma_z^\ell \right) \sigma_x^m, \\ \gamma_{2m} &= \left(\prod_{\ell=1}^{m-1} \sigma_z^\ell \right) \sigma_y^m, \end{aligned} \quad (1)$$

where σ_τ^m , $m = 1, 2, 3$ and $\sigma_\tau = \sigma_x, \sigma_y, \sigma_z$, are Pauli matrices and we have chosen a particular sign convention without physical consequences. The way the three-qubit basis relates to Majorana states is as follows

$$|\mu_1 \mu_2 \mu_3\rangle = (-1)^{\frac{1+\sigma_2}{2}} \prod_{m=1}^3 \left(\frac{\gamma_{2m-1} + i\gamma_{2m}}{2} \right)^{\frac{1+\sigma_m}{2}} |\tilde{0}\rangle, \quad (2)$$

where $\sigma_z^m |\mu_m\rangle = \sigma_m |\mu_m\rangle$, and $|\tilde{0}\rangle \equiv |\downarrow\downarrow\downarrow\rangle$ is the fermionic vacuum.

In the following, we confine ourselves to the 15 physically measurable ‘‘parity’’ observables

$$P_{jk} = i\gamma_j \gamma_k, \quad 1 \leq j < k \leq 6.$$

Parities sharing (not sharing) a common index anti-commute (commute). The total parity operator $\hat{\mathcal{P}} = -i\gamma_1 \gamma_2 \gamma_3 \gamma_4 \gamma_5 \gamma_6$ ($\hat{\mathcal{P}} = -\sigma_z^1 \sigma_z^2 \sigma_z^3$ in the qubit language), commutes with every other parity observable, partitions the full Hilbert space into even ($\mathcal{P} = +1$) and odd ($\mathcal{P} = -1$) parity subspaces. These subspaces are invariant under the action of any parity operator and are isomorphic to logical two-qubit subspaces as illustrated by the mapping of Table I. We use X, Y, Z to denote logical Pauli operators acting on these two-qubit subspaces.

P_{36}	P_{25}	P_{14}	\iff	$\sigma_y^2 \sigma_y^3$	$-\sigma_x^1 \sigma_z^2 \sigma_x^3$	$\sigma_y^1 \sigma_y^2$
P_{12}	P_{34}	P_{56}		$-\sigma_z^1$	$-\sigma_z^2$	$-\sigma_z^3$
P_{45}	P_{16}	P_{23}		$-\sigma_x^2 \sigma_x^3$	$\sigma_y^1 \sigma_z^2 \sigma_y^3$	$-\sigma_x^1 \sigma_x^2$
\iff						
\mathcal{PZZ}			\mathcal{PXX}			\mathcal{PYY}
ZI			IX			\mathcal{PZX}
IZ			XI			\mathcal{PXZ}

TABLE II. (Top) Peres-Mermin-like magic squares using Majorana fermion parity operators and related three physical qubits. Operators in the same row or column commute. (Bottom) The ‘‘emergent’’ operators realize Peres-Mermin magic squares in the (four-dimensional) even-parity ($\mathcal{P} = +1$) or odd-parity ($\mathcal{P} = -1$) subspaces.

We say a set of fermion parity measurements are compatible if the corresponding parity operators are mutually commuting. There are exactly 15 maximal sets of compatible measurements, which are given by

$$\begin{aligned} & \{P_{36}, P_{25}, P_{14}\}, \{P_{12}, P_{34}, P_{56}\}, \{P_{45}, P_{16}, P_{23}\}, \\ & \{P_{36}, P_{12}, P_{45}\}, \{P_{25}, P_{34}, P_{16}\}, \{P_{14}, P_{56}, P_{23}\}, \\ & \{P_{35}, P_{16}, P_{24}\}, \{P_{46}, P_{25}, P_{13}\}, \{P_{12}, P_{35}, P_{46}\}, \\ & \{P_{56}, P_{24}, P_{13}\}, \{P_{46}, P_{15}, P_{23}\}, \{P_{34}, P_{26}, P_{15}\}, \\ & \{P_{36}, P_{24}, P_{15}\}, \{P_{13}, P_{26}, P_{45}\}, \{P_{35}, P_{26}, P_{14}\}. \end{aligned}$$

Product of parities in each set equals the total parity up to a ‘ \pm ’ sign, i.e., if $\{P_{j_1 k_1}, P_{j_2 k_2}, P_{j_3 k_3}\}$ is a maximal set of compatible measurements, then

$$P_{j_1 k_1} P_{j_2 k_2} P_{j_3 k_3} = \pm \hat{\mathcal{P}},$$

where the \pm sign is derived by expressing parities in terms of Majorana operators. We can select the first 6 of those sets and form a 3×3 table which works like a Peres-Mermin magic square^{16,17} up to a unitary equivalence in both even and odd parity subspaces, as illustrated in Table II.

B. Quantum Self-testing

A *self-testing* protocol aims to certify that both an unknown state $|\Psi\rangle$ and a set of unknown measurements are equivalent to an ideal, usually entangled, state $|\hat{\Psi}\rangle$ and a set of ideal measurements. Importantly, the certification does not rely on any assumptions about the state and measurements, other than the assumption that certain pairs of measurement operators commute. The protocol involves repeatedly performing different sets of pairwise commuting measurements. If the ideal measurement statistics are obtained, then the state and measurements are uniquely determined, up to some notion of equivalence. This was first observed by Popescu and Rohrlich¹³, who proved that any state that maximally violates a particular Bell inequality (the CHSH inequality) is equivalent to a singlet state of two qubits. The equivalence is up to a local isometry, because the measurement statistics are unaffected by a local change of basis and by the existence of an auxiliary subsystem on which the measurements act trivially. The notion of self-testing was formalized by Mayers and Yao⁹, and since then, self-testing protocols for many other states and measurement scenarios^{18–23} have been discovered. Such protocols are often called *device-independent* because they rely only on the statistics of measurement outcomes, and not on any physical assumptions about the measurement apparatus.

Two important notions in the self-testing literature are that of *rigidity* and *robustness*. A measurement scenario is rigid if achieving the ideal expectation values uniquely determines the state and measurements, up to a local isometry. In any real experiment, however, the ideal statistics will not be achieved exactly due to errors in the state preparation and measurements. Thus,

any practical self-testing protocol must include a robustness statement. Robustness implies that the state and measurements are still determined approximately if the statistics deviate from the ideal case by a small amount. There are fewer known robustness results for measurements than for states²⁴. Our main results are a rigidity theorem and a robustness theorem for Majorana fermion parity operators.

Our results differ from previous self-testing results in a few respects. First, self-testing scenarios typically involve two or more parties whose measurement operators commute due to a locality assumption. The locality can be physically enforced, for example, by requiring the measurements made by different parties to be spacelike separated. In the scenario we consider, there is no natural notion of locality. Therefore, we do not assume that the full Hilbert space \mathcal{H} factors as a tensor product. Nonetheless, as we show, if the measurement operators have the ideal expectation values, then there is a natural tensor product decomposition. The unknown state $|\Psi\rangle$ is maximally entangled with respect to this emergent tensor product structure. Second, robust self-testing statements are often formulated in terms of an extraction map, which acts on a joint system comprised of the unknown Hilbert space and a reference Hilbert space with a known dimension. In this formulation, a robustness statement asserts that there exists such an extraction map, such that the output state of the reference system has high fidelity with the ideal state^{25,26}. Our theorems avoid using an extraction map and instead directly construct a four-dimensional subspace of \mathcal{H} . In the rigid case, we show that the subspace contains $|\Psi\rangle$ and is invariant under the action of each of the measurement operators. In the case of errors we define an ideal state and ideal operators on the subspace and we lower bound the fidelities of the actual state and measurement operators.

III. STATEMENT OF RESULTS

We consider an experimental setup which ideally involves 6 Majorana modes and 15 parity operators. We imagine an experimentalist who claims to measure fermionic parities of joint Majorana modes. The only thing we are sure about is that some quantum observables are measured, and the minimal assumptions regarding those observables and the state we make in our quantum self-testing protocol are:

1. Our quantum system is prepared repeatedly in some unknown pure state $|\Psi\rangle$.
2. A set of 15 unknown measurement observables, each of which is given by a Hermitian operator A_r , with r denoting a pair of indices (j, k) of putative Majorana modes, satisfying $A_r^2 = \mathbb{1}$. Such operators are oftentimes called Hermitian involutions.
3. We assume that $[A_r, A_s] = 0$ whenever r and s do not share a common index.

The first assumption can be relaxed to consider an unknown mixed state ρ , but since any mixed state has a pure state extension, we can take $\rho = |\Psi\rangle\langle\Psi|$ to be pure without loss of generality. Similarly, we can relax the second and third assumptions and consider each measurement to be an unknown two-outcome generalized measurement (positive operator-valued measure or POVM) $Q_r = \{Q_{r,0}, Q_{r,1}\}$, satisfying $Q_{r,a} \geq 0$ and $Q_{r,0} + Q_{r,1} = \mathbb{1}$, along with $[Q_{r,a}, Q_{s,b}] = 0$, $a, b = 0, 1$, whenever r and s do not share a common index. However, our assumption of Hermitian observables is also without loss of generality, as we prove in Appendix B that the POVMs Q_r can be extended to orthogonal projective measurements with the same pairwise commutativity structure as the POVMs. We emphasize that no other assumptions about the state or measurements are made. In particular, we do not assume the dimension, or particular tensor or non-tensor product structures, of the Hilbert space \mathcal{H} . In this paper, we aim to infer Majorana behavior, e.g., the anti-commutation relation between claimed Majorana fermions and their parity observables, solely from the statistics of measurement outcomes using the quantum self-testing method defined in Sec. II B.

These 15 A_r operators can be visualized as edges on K_6 , the complete graph on 6 vertices, as shown in Fig. 1. The vertices correspond to putative Majorana modes, and two operators commute if their associated edges do not share a common index. When convenient, we will use a double index as in A_{jk} to denote the operator associated with edge (j, k) . The maximal sets of commuting observables are given by perfect matchings on K_6 .

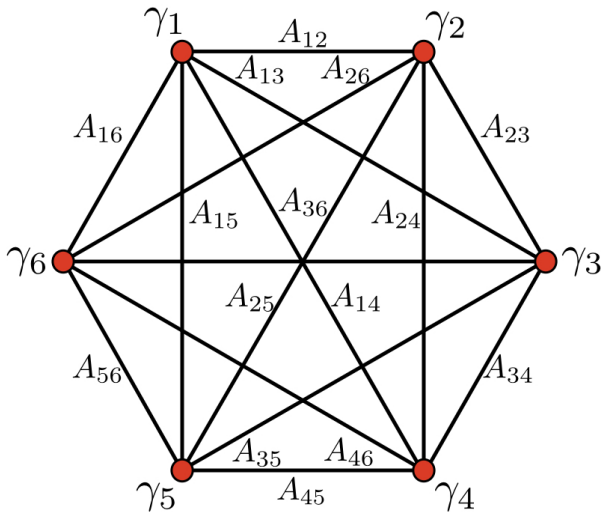


FIG. 1. Six Majorana fermion modes γ_l indicated by 6 vertices. Each edge in the K_6 graph represents a claimed Majorana fermion parity measurement A_{jk} between γ_l and γ_k .

Our self-testing theorems apply to any set of six parities corresponding to a cycle subgraph $G \subseteq K_6$. For concreteness, we take G to be the cycle whose edge set

is $E = \{(1, 2), (2, 3), (3, 4), (4, 5), (5, 6), (1, 6)\}$. We refer to a maximal set of commuting parity operators in G as a *context*. We arrange the six unknown operators into a 2-by-3 table where the operators in each row and column form a context (see Table III (Left)). Any two operators A_r and A_s not in the same row or column correspond to edges r and s that are adjacent in G , which we denote $r \sim s$. The ideal fermionic parity operators corresponding to adjacent edges anti-commute. Since 6 Majorana modes acting on a given parity (even or odd) sector encode 2 logical qubits, the ideal operators can be any set of 6 logical two-qubit Pauli operators with the ideal commutation and anti-commutation relations. For concreteness, we fix a basis in which the ideal operators are as in Table III (Right).

$$\begin{array}{|c|c|c|} \hline A_{12} & A_{34} & A_{56} \\ \hline A_{45} & A_{16} & A_{23} \\ \hline \end{array} \iff \begin{array}{|c|c|c|} \hline ZI & IX & ZX \\ \hline IZ & XI & XZ \\ \hline \end{array}$$

TABLE III. (Left) The six unknown operators and five contexts. (Right) The six “emergent” logical two-qubit Pauli operators.

Let \mathcal{R}_i and \mathcal{C}_i be the sets of edges in the i th row and column, respectively. The *ideal expectations* in our self-testing protocol are the following expectation values of products of observables in each context:

$$\begin{aligned} \langle\Psi| \prod_{r \in \mathcal{R}_i} A_r |\Psi\rangle &= 1 \quad i \in \{1, 2\}, \\ \langle\Psi| \prod_{r \in \mathcal{C}_i} A_r |\Psi\rangle &= \begin{cases} 1, & i \in \{1, 2\} \\ -1, & i = 3. \end{cases} \end{aligned} \quad (3)$$

The ideal expectations are achieved by the ideal state $|\hat{\Psi}\rangle = \frac{1}{\sqrt{2}}(|00\rangle + |11\rangle)$. We remark that our particular definition of the ideal expectations is a choice of convention. A similar rigidity result for a different ideal state follows from any similar set of ideal expectations where an odd number of contexts have an expectation value of -1 .

Let \mathcal{A} be the algebra generated by $\{A_r : r \in G\}$, and $V \subseteq \mathcal{H}$ be the subspace defined by $V = \text{span}\{A|\Psi\rangle : A \in \mathcal{A}\}$. Let P be the projector onto V , and $\mathbb{A}_r = PA_rP$.

Theorem 1 (Rigidity of Majorana Parities). *If the ideal expectations are satisfied, then V is a 4-dimensional subspace and $\{\mathbb{A}_r, \mathbb{A}_s\} = 0$, for all $r, s \in G$ with $r \sim s$. Furthermore, the state $|\Psi\rangle$ satisfies $\prod_{r \in \mathcal{C}_i} A_r |\Psi\rangle = \pm |\Psi\rangle$. Here, “ $-$ ” should be understood only for \mathcal{C}_3 .*

The proof of the theorem given in the next section. As a consequence of Theorem 1, a basis for V can be chosen in which the operators on the (Left) in Table III equal those on the (Right) of the same Table III, and $|\Psi\rangle = |\hat{\Psi}\rangle$.

In practice, experimental measurements do not satisfy the ideal expectations due to imperfections in the state preparation and measurements. We say that the ideal

expectations are satisfied to within error ϵ if

$$\begin{aligned} \langle \Psi | \prod_{r \in \mathcal{R}_i} A_r | \Psi \rangle &\geq 1 - \epsilon \quad i \in \{1, 2\}, \\ \pm \langle \Psi | \prod_{r \in \mathcal{C}_i} A_r | \Psi \rangle &\geq 1 - \epsilon \quad i \in \{1, 2, 3\}, \end{aligned} \quad (4)$$

where the minus sign in the second line is used for the third column only. In the presence of errors, the subspace V is no longer invariant under the action of the operators A_r . However, the protocol is still robust in the following sense. There exists an ideal subspace \hat{V} of dimension 4, along with an ideal state $|\hat{\Psi}\rangle$ and ideal operators \hat{A}_r whose fidelities with respect to the actual state and operators are close to 1, within errors linear in ϵ . Here the state fidelity is $F(|\hat{\Psi}\rangle, |\Psi\rangle) = |\langle \hat{\Psi} | \Psi \rangle|^2$, and the operator fidelity is defined as $F(\hat{A}_r, A_r) = \frac{1}{4} \text{Tr}(\hat{A}_r A_r)$. Formally, we have the following:

Theorem 2 (Protocol Robustness). *If the ideal expectations are satisfied within error ϵ , then there exists $\hat{V} \subseteq \mathcal{H}$, with $\dim(\hat{V}) = 4$, Hermitian involutions $\hat{A}_r : \hat{V} \rightarrow \hat{V}$ for each $r \in G$ such that $\{\hat{A}_r, \hat{A}_s\} = 0$ if $r \sim s$ and $[\hat{A}_r, \hat{A}_s] = 0$ otherwise, and a state $|\hat{\Psi}\rangle \in \hat{V}$ such that $\prod_{r \in \mathcal{C}_i} \hat{A}_r |\hat{\Psi}\rangle = |\hat{\Psi}\rangle$ for $i \in \{1, 2\}$, and such that they satisfy*

$$\begin{aligned} F(|\hat{\Psi}\rangle, |\Psi\rangle) &\geq 1 - \epsilon_0, \\ F(\hat{A}_r, A_r) &\geq 1 - \epsilon_i, \quad \text{for } r \in \mathcal{C}_i, \end{aligned}$$

where $\epsilon_0 = 14\epsilon$, $\epsilon_1 = 0$, $\epsilon_2 = 25\epsilon/2$, and $\epsilon_3 = (\sqrt{2} + \sqrt{14 + \sqrt{44}})^2 \epsilon/2 \simeq 69.5\epsilon$.

The proof of the above theorem is given in Sec. V, with some details deferred to Appendix D and E. The perfect fidelity of the first column operators is due to a choice of basis. For simplicity, we have chosen our error bounds to be equal. Our results can be generalized to the case of unequal errors for different contexts, however, we do not carry out this analysis here.

IV. RIGIDITY OF MAJORANA FERMION PARITY MEASUREMENTS

This section deals with the situation where ideal statistics is satisfied, and proves Theorem 1. Our Lemma 3 shows that operators with adjacent edges anti-commute exactly in their action on $|\Psi\rangle$, a smoking gun for Majorana detection.

Since each A_r has eigenvalues in $\{-1, +1\}$, the ideal expectations are satisfied only if $|\Psi\rangle$ is a ± 1 eigenstate of the products of operators in each context.

$$\begin{aligned} \prod_{r \in \mathcal{R}_i} A_r |\Psi\rangle &= |\Psi\rangle \quad i \in \{1, 2\}, \\ \prod_{r \in \mathcal{C}_i} A_r |\Psi\rangle &= \pm |\Psi\rangle \quad i \in \{1, 2, 3\}, \end{aligned}$$

where again the minus sign in the last equation is for column 3 only. Using the fact that $A_r^2 = \mathbb{1}$, and the commutativity of operators in each context, we can move operators freely between the left and right sides of the above equations. For example, the identities

$$\begin{aligned} A_{12} A_{34} |\Psi\rangle &= A_{56} |\Psi\rangle, \\ A_{34} |\Psi\rangle &= A_{16} |\Psi\rangle, \end{aligned}$$

hold for row 1 and column 2, respectively.

Lemma 3. *Suppose the ideal expectations are satisfied. Then $\{A_r, A_s\} |\Psi\rangle = 0$, for $r \sim s$.*

Proof. We show that $\{A_{12}, A_{16}\} |\Psi\rangle = 0$. Making repeated use of identities such as the ones above, we compute

$$\begin{aligned} A_{12} A_{16} |\Psi\rangle &= A_{12} A_{34} |\Psi\rangle = A_{56} |\Psi\rangle \\ &= -A_{23} |\Psi\rangle = -A_{16} A_{12} |\Psi\rangle = -A_{16} A_{12} |\Psi\rangle. \end{aligned}$$

By symmetry of the table, a similar argument shows that the same relation holds for any A_r and A_s with $r \sim s$. \square

We now construct a subspace and show that it is invariant under the action of \mathcal{A} . Define $V' \subseteq \mathcal{H}$ by

$$V' = \text{span}\{|\Psi\rangle, A_{12} |\Psi\rangle, A_{16} |\Psi\rangle, A_{12} A_{16} |\Psi\rangle\}.$$

Lemma 4. *$A_r V' \subseteq V'$ for all $r \in G$.*

Proof. Since $A_{12}^2 = \mathbb{1}$, $A_{12} V' \subseteq V'$. To see that $A_{16} V' \subseteq V'$, note that Lemma 3 implies $A_{16} A_{12} |\Psi\rangle = -A_{12} A_{16} |\Psi\rangle$ and $A_{16} A_{12} A_{16} |\Psi\rangle = -A_{12} |\Psi\rangle$. We next check that $A_{34} V' \subseteq V'$. This follows from $A_{34} |\Psi\rangle = A_{16} |\Psi\rangle$, and from the fact that A_{34} commutes with A_{16} and A_{12} . By symmetry of the table, we also have that $A_{45} V' \subseteq V'$. It remains to show that A_{56} and A_{23} act invariantly on V' . Explicitly,

$$\begin{aligned} A_{56} |\Psi\rangle &= A_{12} A_{34} |\Psi\rangle \in V' \\ A_{56} A_{12} |\Psi\rangle &= A_{12} A_{56} |\Psi\rangle \in V' \\ A_{56} A_{16} |\Psi\rangle &= A_{56} A_{34} |\Psi\rangle = A_{12} |\Psi\rangle \in V' \\ A_{56} A_{12} A_{16} |\Psi\rangle &= A_{56} A_{12} A_{34} |\Psi\rangle = |\Psi\rangle \in V'. \end{aligned}$$

Similarly, by symmetry, we also have $A_{23} V' \subseteq V'$. \square

Having shown that V' is an invariant subspace, it follows that $V' = V = \mathcal{A} |\Psi\rangle$. We can now work with the operators restricted onto V . Let $\mathbb{A}_r = P A_r P$, with P the projector onto V . Note that $AP = PAP$ for all $A \in \mathcal{A}$. The next Lemma states that commutativity and anti-commutativity of operators on a full Hilbert space is preserved under restriction onto a subspace.

Lemma 5. *Let A and B be Hermitian involutions, and let P be a projector such that $AP = PAP$. Then*

$$\begin{aligned} [A, B] = 0 &\implies [PAP, PBP] = 0, \\ \{A, B\} = 0 &\implies \{PAP, PBP\} = 0. \end{aligned}$$

Proof. $(PAP)(PBP) = PAPBP = (PAP)^\dagger BP = (AP)^\dagger BP = PABP = \pm PBAP = \pm PBPAP = \pm(PBP)(PAP)$, with the plus or minus sign depending on whether A and B commute or anti-commute, respectively. \square

We are now ready to prove Theorem 1.

Proof of Theorem 1. We first determine the action on V of the operators in \mathcal{C}_1 and \mathcal{C}_2 . From Lemma 5, both \mathbb{A}_{12} and \mathbb{A}_{16} commute with both \mathbb{A}_{34} and \mathbb{A}_{45} , and therefore

$$[\mathbb{A}_{12}\mathbb{A}_{16}, \mathbb{A}_{45}\mathbb{A}_{34}] = 0.$$

Since $\mathbb{A}_{jk}^2 = P$, $\mathbb{A}_{12}\mathbb{A}_{16}$ and $\mathbb{A}_{45}\mathbb{A}_{34}$ are unitary on V . Therefore, there exists an orthogonal basis for V of simultaneous eigenstates of $\mathbb{A}_{12}\mathbb{A}_{16}$ and $\mathbb{A}_{45}\mathbb{A}_{34}$. Let $|\alpha, \beta\rangle$ be one such eigenstate satisfying

$$\begin{aligned} \mathbb{A}_{12}\mathbb{A}_{16} |\alpha, \beta\rangle &= \alpha |\alpha, \beta\rangle, \\ \mathbb{A}_{34}\mathbb{A}_{45} |\alpha, \beta\rangle &= \beta |\alpha, \beta\rangle, \end{aligned}$$

and also satisfying $\langle \alpha, \beta | \Psi \rangle \neq 0$. Such a state exists since $|\Psi\rangle \in V$. From Lemma 3, $\{\mathbb{A}_{12}, \mathbb{A}_{16}\} |\Psi\rangle = 0$, and hence $\{\mathbb{A}_{12}, \mathbb{A}_{16}\} |\Psi\rangle = 0$ by Lemma 5. Similarly, $\{\mathbb{A}_{34}, \mathbb{A}_{45}\} |\Psi\rangle = 0$. These two equations imply $\alpha + \bar{\alpha} = 0$ and $\beta + \bar{\beta} = 0$, and thus $\alpha, \beta \in \{i, -i\}$, where $\bar{\alpha}$ denotes the complex conjugation of α .

Now, define $|\bar{\alpha}, \beta\rangle = \mathbb{A}_{12} |\alpha, \beta\rangle$. Note that $\mathbb{A}_{12}\mathbb{A}_{16}(\mathbb{A}_{12} |\alpha, \beta\rangle) = \mathbb{A}_{12}(\mathbb{A}_{12}\mathbb{A}_{16})^\dagger |\alpha, \beta\rangle = \bar{\alpha} \mathbb{A}_{12} |\alpha, \beta\rangle$, and therefore

$$\mathbb{A}_{12}\mathbb{A}_{16} |\bar{\alpha}, \beta\rangle = \bar{\alpha} |\bar{\alpha}, \beta\rangle.$$

Similarly, defining $|\alpha, \bar{\beta}\rangle = \mathbb{A}_{45} |\alpha, \beta\rangle$, and $|\bar{\alpha}, \bar{\beta}\rangle = \mathbb{A}_{12}\mathbb{A}_{45} |\alpha, \beta\rangle$, we see that $|\alpha, \beta\rangle$, $|\alpha, \bar{\beta}\rangle$, $|\bar{\alpha}, \beta\rangle$, and $|\bar{\alpha}, \bar{\beta}\rangle$ are joint eigenstates of $\mathbb{A}_{12}\mathbb{A}_{16}$ and $\mathbb{A}_{45}\mathbb{A}_{34}$ with eigenvalues (α, β) , $(\alpha, \bar{\beta})$, $(\bar{\alpha}, \beta)$, and $(\bar{\alpha}, \bar{\beta})$, respectively. These eigenstates are pairwise orthogonal, since $\alpha, \beta \in \{i, -i\}$. Therefore, V is a 4-dimensional subspace. Next, note that

$$\begin{aligned} \mathbb{A}_{16}\mathbb{A}_{12} |\alpha, \beta\rangle &= (\mathbb{A}_{12}\mathbb{A}_{16})^\dagger |\alpha, \beta\rangle = \bar{\alpha} |\alpha, \beta\rangle \\ &= -\alpha |\alpha, \beta\rangle = -\mathbb{A}_{12}\mathbb{A}_{16} |\alpha, \beta\rangle \end{aligned}$$

Similar calculations applied to the remaining eigenstates of $\mathbb{A}_{12}\mathbb{A}_{16}$ and $\mathbb{A}_{34}\mathbb{A}_{45}$ show that $\{\mathbb{A}_{12}, \mathbb{A}_{16}\} = 0$ and $\{\mathbb{A}_{45}, \mathbb{A}_{34}\} = 0$. Therefore, there is a basis for V in which

$$\begin{aligned} \mathbb{A}_{12} &= ZI, & \mathbb{A}_{34} &= IX, \\ \mathbb{A}_{45} &= IZ, & \mathbb{A}_{16} &= XI. \end{aligned}$$

We work in this basis for the remainder of the proof. The next step is to determine $|\Psi\rangle$. From $\mathbb{A}_{12}\mathbb{A}_{45} |\Psi\rangle = ZZ |\Psi\rangle = |\Psi\rangle$, and $\mathbb{A}_{34}\mathbb{A}_{16} |\Psi\rangle = XX |\Psi\rangle = |\Psi\rangle$, it follows that

$$|\Psi\rangle = \frac{1}{\sqrt{2}}(|00\rangle + |11\rangle).$$

The final step is to determine \mathbb{A}_{56} and \mathbb{A}_{23} . We begin with \mathbb{A}_{56} . Since $[A_{56}, A_{12}] = 0 = [A_{56}, A_{34}]$, Lemma 5 implies that $[\mathbb{A}_{56}, \mathbb{A}_{12}] = 0 = [\mathbb{A}_{56}, \mathbb{A}_{34}]$. Therefore, when expanded in a basis of two-qubit Pauli matrices, \mathbb{A}_{56} can only have non-zero weight on II, ZI, IX , and ZX . However, $\mathbb{A}_{56} |\Psi\rangle = \mathbb{A}_{12}\mathbb{A}_{34} |\Psi\rangle = ZX |\Psi\rangle$, which implies $\mathbb{A}_{56} = ZX$, since the states $|\Psi\rangle, XI |\Psi\rangle, IX |\Psi\rangle$, and $ZX |\Psi\rangle$ are pairwise orthogonal. Similarly, using $[\mathbb{A}_{23}, \mathbb{A}_{45}] = 0 = [\mathbb{A}_{23}, \mathbb{A}_{16}]$ and $\mathbb{A}_{23} |\Psi\rangle = \mathbb{A}_{45}\mathbb{A}_{26} |\Psi\rangle$, it follows that $\mathbb{A}_{23} = XZ$. \square

V. ROBUSTNESS TO ERRORS

We now consider the situation where the ideal statistics are satisfied to within error ϵ . We first prove an approximate version of Lemma 3.

Lemma 6. *Suppose the ideal expectations are satisfied to within error ϵ . Then $\|\{A_r, A_s\} |\Psi\rangle\| \leq 5\sqrt{2}\epsilon$ for all $r, s \in G$ with $r \sim s$.*

Proof. We show that $\|\{A_{12}, A_{16}\} |\Psi\rangle\| \leq 5\sqrt{2}\epsilon$. For r and s in the same column,

$$\begin{aligned} \|A_r |\Psi\rangle \pm A_s |\Psi\rangle\| &= \sqrt{2(1 \pm \langle \Psi | A_r A_s | \Psi \rangle)} \\ &\leq \sqrt{2(1 - (1 - \epsilon))} \\ &= \sqrt{2\epsilon}, \end{aligned} \quad (5)$$

where in the first line, the plus sign is used for column 3, and the minus sign for columns 1 and 2. Similarly, for both rows of the table, with r, s , and t in the same row,

$$\|A_r |\Psi\rangle - A_s A_t |\Psi\rangle\| \leq \sqrt{2\epsilon}. \quad (6)$$

Therefore, by a chain of triangle inequalities, and using the fact that $\|U |\Psi\rangle\| = \|\Psi\rangle\|$ for any unitary U ,

$$\begin{aligned} \|(\mathbb{A}_{12}\mathbb{A}_{16} + \mathbb{A}_{16}\mathbb{A}_{12}) |\Psi\rangle\| &\leq \|(\mathbb{A}_{12}\mathbb{A}_{16} - \mathbb{A}_{12}\mathbb{A}_{34}) |\Psi\rangle\| \\ &\quad + \|(\mathbb{A}_{12}\mathbb{A}_{34} - \mathbb{A}_{56}) |\Psi\rangle\| + \|(\mathbb{A}_{56} + \mathbb{A}_{23}) |\Psi\rangle\| \\ &\quad + \|(-\mathbb{A}_{23} + \mathbb{A}_{16}\mathbb{A}_{45}) |\Psi\rangle\| + \|(-\mathbb{A}_{16}\mathbb{A}_{45} + \mathbb{A}_{16}\mathbb{A}_{12}) |\Psi\rangle\| \\ &\leq 5\sqrt{2}\epsilon. \end{aligned}$$

Using a similar argument for any $r \sim s$, one can prove $\|\{A_r, A_s\} |\Psi\rangle\| \leq 5\sqrt{2}\epsilon$. \square

By a corollary to Jordan's Lemma, which we prove in Appendix C, \mathcal{H} decomposes as $\mathcal{H} = \bigoplus_l \mathcal{H}_l$, where each \mathcal{H}_l is 4-dimensional and invariant under the action of A_{12}, A_{16}, A_{34} , and A_{45} . Since both of A_{12}, A_{16} commute with both of A_{34}, A_{45} , each invariant subspace \mathcal{H}_l in the Jordan decomposition factors as a tensor product of two qubits. Therefore, there is a basis for each subspace such that

$$\begin{aligned} A_{12} &= \bigoplus_l ZI, & A_{34} &= \bigoplus_l (\cos \phi_l IX + \sin \phi_l IZ), \\ A_{45} &= \bigoplus_l IZ, & A_{16} &= \bigoplus_l (\cos \theta_l XI + \sin \theta_l ZI), \end{aligned} \quad (7)$$

with $\theta_l, \phi_l \in [-\frac{\pi}{2}, \frac{\pi}{2}]$. Label this chosen basis for each \mathcal{H}_l as $\{|00_l\rangle, |01_l\rangle, |10_l\rangle, |11_l\rangle\}$.

Next, with respect to this Jordan decomposition, one can write $|\Psi\rangle$ as

$$|\Psi\rangle = \sum_l \sqrt{p_l} |\Psi_l\rangle,$$

where each $|\Psi_l\rangle \in \mathcal{H}_l$ and $\sum p_l = 1$. We define the ideal subspace \hat{V} as the linear span

$$\hat{V} = \text{span}\{|ab\rangle = \sum_l \sqrt{p_l} |ab_l\rangle : a, b \in \{0, 1\}\}.$$

We define the ideal operators to be logical Pauli product operators in the above basis. Specifically, $\hat{A}_{12} = ZI$, $\hat{A}_{34} = IX$, $\hat{A}_{56} = ZX$, $\hat{A}_{45} = IZ$, $\hat{A}_{16} = XI$, $\hat{A}_{23} = XZ$. Finally, we define the ideal state with respect to the above basis as

$$|\hat{\Psi}\rangle = \frac{|00\rangle + |11\rangle}{\sqrt{2}}. \quad (8)$$

Proof of Theorem 2. By definition, $\{\hat{A}_r, \hat{A}_s\} = 0$ for $r, s \in G$ with $r \sim s$, and the ideal state satisfies $\prod_{r \in \mathcal{C}_i} \hat{A}_r |\hat{\Psi}\rangle = |\hat{\Psi}\rangle$ for $i \in \{1, 2\}$.

We first calculate the state fidelity. Define $|\hat{\Psi}_l\rangle = \frac{1}{\sqrt{2}}(|00_l\rangle + |11_l\rangle)$. Using the freedom to choose the overall phase in each subspace, we set $\langle \hat{\Psi}_l | \Psi_l \rangle \geq 0$. Therefore,

$$\langle \hat{\Psi} | \Psi \rangle = \sum_l p_l \langle \hat{\Psi}_l | \Psi_l \rangle \geq \sum_l p_l |\langle \hat{\Psi}_l | \Psi_l \rangle|^2.$$

It will be convenient to work in the Y basis $\{|0_Y 0_Y\rangle, |0_Y 1_Y\rangle, |1_Y 0_Y\rangle, |1_Y 1_Y\rangle\}$ within each Jordan subspace \mathcal{H}_l . Here $|0_Y\rangle = (|0\rangle + i|1\rangle)/\sqrt{2}$, and $|1_Y\rangle = (|0\rangle - i|1\rangle)/\sqrt{2}$. We expand $|\Psi_l\rangle$ as

$$|\Psi_l\rangle = \sum_{a,b \in \{0,1\}} c_{ab}^l |a_Y b_Y\rangle,$$

where $\sum_{a,b} |c_{ab}^l|^2 = 1$. In this basis, the ideal state is

$$|\hat{\Psi}\rangle = \sum_l \sqrt{\frac{p_l}{2}} (|0_Y 1_Y\rangle + |1_Y 0_Y\rangle).$$

Therefore,

$$\begin{aligned} \langle \hat{\Psi} | \Psi \rangle &\geq \sum_l p_l |\langle \hat{\Psi}_l | \Psi_l \rangle|^2 \\ &= \sum_l p_l \frac{1}{2} |c_{01}^l + c_{10}^l|^2 \\ &= \sum_l p_l (|c_{01}^l|^2 + |c_{10}^l|^2 - \frac{1}{2} |c_{01}^l - c_{10}^l|^2) \\ &= 1 - \sum_l p_l (|c_{00}^l|^2 + |c_{11}^l|^2) - \sum_l p_l \frac{1}{2} |c_{01}^l - c_{10}^l|^2 \end{aligned}$$

In Appendix D, we prove that

$$\sum_l p_l (|c_{00}^l|^2 + |c_{11}^l|^2) \leq \frac{13}{2} \epsilon, \quad (9)$$

$$\sum_l p_l |c_{01}^l - c_{10}^l|^2 \leq \epsilon. \quad (10)$$

Thus, the state fidelity is bounded according to

$$\begin{aligned} F(|\hat{\Psi}\rangle, |\Psi\rangle) &\geq (1 - 7\epsilon)^2 \\ &\geq 1 - 14\epsilon. \end{aligned} \quad (11)$$

Next we bound the fidelity of the operators, starting with the first column. From Eq. (7) and the definition of the ideal operators, for $r \in \mathcal{C}_1$, $\text{Tr}(\hat{A}_r A_r) = 4$ and so $F(\hat{A}_r, A_r) = 1$. For the second column, Eq. (7) implies

$$F(\hat{A}_{16}, A_{16}) = \sum_l p_l \cos \theta_l.$$

Combining Lemma 6 with Eq. (7),

$$\begin{aligned} \frac{25}{2} \epsilon &\geq \frac{1}{4} \|\{A_{12}, A_{16}\} |\Psi\rangle\|^2 \\ &= \sum_l p_l \sin^2 \theta_l \\ &= 1 - \sum_l p_l \cos^2 \theta_l \\ &\geq 1 - \sum_l p_l \cos \theta_l. \end{aligned} \quad (12)$$

where the last line follows from $\theta_l \in [-\frac{\pi}{2}, \frac{\pi}{2}]$ and therefore $\cos \theta_l \geq 0$. Combining the last two equations yields

$$F(\hat{A}_{16}, A_{16}) \geq 1 - \frac{25}{2} \epsilon.$$

A similar calculation shows that $F(\hat{A}_{23}, A_{23}) \geq 1 - \frac{25}{2} \epsilon$ also.

The final step is to bound the fidelities of the third column operators. We begin with A_{56} . The ϵ error in the first row implies

$$\|A_{12} A_{34} |\Psi\rangle - A_{56} |\Psi\rangle\| \leq \sqrt{2\epsilon}, \quad (13)$$

and from the state fidelity, Eq. (11), we get

$$\|A_{56} (|\Psi\rangle - |\hat{\Psi}\rangle)\| = \|\Psi\rangle - |\hat{\Psi}\rangle\| \leq \sqrt{14\epsilon}. \quad (14)$$

We show in Appendix E that

$$\|\hat{A}_{34} |\hat{\Psi}\rangle - A_{34} |\Psi\rangle\| \leq \sqrt{44\epsilon}. \quad (15)$$

Applying the triangle inequality to Eqs. (13)-(15), and using $\hat{A}_{12} = A_{12}$,

$$\|\hat{A}_{12} \hat{A}_{34} |\hat{\Psi}\rangle - A_{56} |\hat{\Psi}\rangle\| \leq (\sqrt{2} + \sqrt{14} + \sqrt{44}) \sqrt{\epsilon},$$

which implies

$$\text{Re}\langle\hat{\Psi}|\hat{A}_{12}\hat{A}_{34}A_{56}|\hat{\Psi}\rangle \geq 1 - \epsilon_3.$$

Since $[A_{12}, A_{56}] = 0$ and $\hat{A}_{12}^2 = P$, Lemma 5 implies $[\hat{A}_{12}, A_{56}] = 0$. Therefore, when expanded in a basis of two-qubit Pauli matrices, A_{56} can only have I or Z acting on the first qubit. Since $A_{12}\hat{A}_{34} = ZX$, only the ZX component of A_{56} contributes to $\text{Re}\langle\hat{\Psi}|\hat{A}_{12}\hat{A}_{34}A_{56}|\hat{\Psi}\rangle$, as any other component either gives zero or a purely imaginary number. Hence,

$$\begin{aligned} \text{Re}\langle\hat{\Psi}|\hat{A}_{12}\hat{A}_{34}A_{56}|\hat{\Psi}\rangle &= \text{Re}\langle\hat{\Psi}|\hat{A}_{56}A_{56}|\hat{\Psi}\rangle \\ &= \frac{1}{4} \text{Tr}\left(\hat{A}_{56}A_{56}\right) \\ &= F(\hat{A}_{56}, A_{56}), \end{aligned}$$

and it follows that $F(\hat{A}_{56}, A_{56}) \geq 1 - \epsilon_3$. By a similar argument one can show that $F(\hat{A}_{23}, A_{23}) \geq 1 - \epsilon_3$. \square

VI. DISCUSSION AND OUTLOOK

We have shown that measurements of Majorana fermion parities can be self-tested. This fact provides a powerful tool for determining how consistent experimental data is with the existence of Majorana fermion modes. Experimentally, our protocol requires the ability to measure 6 observables A_{jk} , which ideally correspond to parities P_{jk} between consecutive Majorana modes.

A hypothetical experimental setup is shown in Fig 2; an actual implementation may involve a more complex geometry or even multiple quantum dots for fermion parity measurements. We are interested in platforms similar to the ones described in Ref. [12] in which nanoscale topological superconducting (because of the proximity effect) wires are utilized. Quasiparticle poisoning can be suppressed by performing measurements at temperatures T lower than the superconducting gap Δ . To avoid errors due to the splitting of the ground state degeneracy, leading to non well-defined Majorana modes, we must choose the length of the nanowire L long enough compared to the effective coherence length ξ , i.e., $L \gg \xi$. Also, we need to suppress the charging energy E_C between wires to avoid couplings that also split the degeneracy of the ground state in each wire. Fermion parities A_{jk} are measured by selectively coupling nanowires j and k to the quantum dot with a tunneling amplitude $t_{j,k}$ such that $|t_{j,k}| \ll \Delta$, controlled by gates, which is exponentially suppressed in the tunnel barrier because of the superconducting gap.

The expectation value of any context (set of observables in a row or column of Table III (Left)) can be obtained by repeatedly preparing a specific initial state, measuring the operators in that context, and using Eqs. (A1) and (A2). Given data from the measurements in each context, we can express the result by an operator W , often called a contextuality witness in the quantum

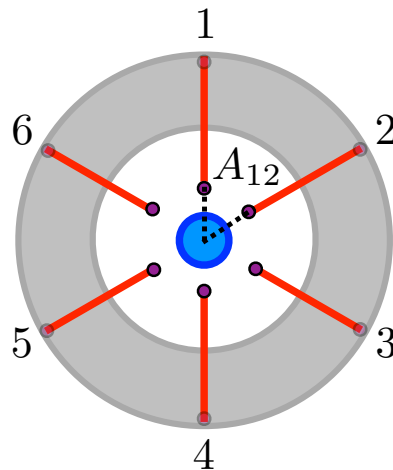


FIG. 2. Possible experimental setup to measure Majorana fermion parities A_{jk} with eigenvalues $a_{jk} = \pm 1$. Six (topological) semiconducting (e.g., InAs) wires in proximity to a superconductor (indicated as a grey annulus) and a quantum dot in the center where parities are measured.

information literature,

$$\begin{aligned} W &= A_{12}A_{34}A_{56} + A_{45}A_{16}A_{23} \\ &\quad + A_{12}A_{45} + A_{34}A_{16} - A_{56}A_{23}. \end{aligned} \quad (16)$$

The witness is not unique, as different choices of the initial state result in different combinations of signs of the terms in W , according to Table V in Appendix A.

For a fixed total parity (odd or even), 6 Majorana fermions theoretically encode a two qubit subspace, where each qubit is encoded non-locally in 3 Majorana modes in Fig. 2. An experimental outcome $\langle W \rangle \leq 3$ implies classical assignments of outcomes to the measured observables and the impossibility of realizing a Majorana topological qubit. Our result, Theorem 1, implies that the maximal value predicted by quantum mechanics, i.e. $\langle W \rangle = 5$ is obtained *only* if the observables corresponding to adjacent parities anti-commute. However, experimental outcomes carry some errors in practice, either due to the fact that the state has a component in an excited state or because of imperfect tuning of the measurement parameters. Theorem 2, in turn, accounts for those errors in the experimental outcomes. Essentially, it establishes rigorous lower bounds on the fidelities of the state and measurement operators that are linear in the errors, implying that a small error certifies that each A_{jk} may have high fidelity with the corresponding hypothetical fermion parity operator. For example, in a basis where the parities in the first row are perfect, a 0.1% error in the expectation value of each context implies upper bounds on the error of the second and third column operators of 1.25% and 6.95%. Therefore, a small error in the expectation value of contexts implies that quantum error correction may still be operative.

We emphasize that although our proposal is to self-test

parities in Majorana modes, our protocol can be simulated in other physical systems via the Jordan-Wigner mapping given by Eq. (1) and Table II. Examples include trapped ions, where product of Pauli operators can be measured with global entangling gates and the use of an ancilla²⁷, or also neutron beams entangled in energy, path and spin degrees of freedom^{28,29}. These extended simulations may seem strange at first reading. Note that our assumptions in Sec. III do not restrict measurements to be local in the physical operator language representation. Our protocol tests the topological property of Majorana modes because fermion parity measurements are local in the physical representation. Equivalent measurements in the spin language representation would be non-local as Table II indicates. Additionally, the required measurements in, for example, ion systems are not compatible for arbitrary contexts, without making additional assumptions, since those measurements are not necessarily performed on separable subsystems. On the other hand, compatibility in the Majorana fermion case is justified because of spatial separability. A main contribution of our work is the development of robust self-testing protocols assuming only compatibility among observables in each context rather than a tensor product factorization of the Hilbert space.

We conclude with some open problems and suggestions for future work. The robustness bounds in our Theorem 2 are certainly not tight, which raises the question of how much they can be improved. It might be possible to obtain a stronger robustness statement using different methods such as those based on a semidefinite

programming hierarchy^{30,31}, or linear operator inequalities²⁰. How does our formulation of robustness by constructing an ideal subspace relate to the notion of robustness as measured by an extraction map? Finally, while our protocol certifies a single state and a set of measurements, gates in topological quantum computing are implemented by braiding. It is therefore desirable to extend the protocol to include a self-test of braiding operations.

We strongly believe that certification of quantum measurements in various physical scenarios is a promising technique for precision measurement and quantum validation. We anticipate generalizations of our current approach to many other situations of physical interest exploring the frontiers of quantum mechanics.

ACKNOWLEDGMENTS

GO would like to acknowledge partial support by the DOE grant DE-SC0020343. This research was conducted in part under the PREP program with financial assistance from U.S. Department of Commerce, National Institute of Standards and Technology. Contributions to this article by workers at the National Institute of Standards and Technology, an agency of the U.S. Government, are not subject to U.S. copyright. The authors thank Scott Glancy and Carl Miller for reviewing an early draft of this paper.

* These authors contributed equally to this work.

¹ J. Alicea, “New directions in the pursuit of majorana fermions in solid state systems,” *Rep. Prog. Phys.* **75**, 076501 (2012).

² E. Majorana, “Theory of the symmetry of electrons and positrons,” *Nuovo Cim.* **14**, 171 (1937).

³ V. Mourik *et al.*, “Signatures of majorana fermions in hybrid superconductor-semiconductor nanowire devices,” *Science* **336**, 1003 (2012).

⁴ L. P. Rokhinson, X. Liu, and J. K. Furdyna, “The fractional a.c. josephson effect in a semiconductor-superconductor nanowire as a signature of majorana particles,” *Nat. Phys.* **8**, 795 (2012).

⁵ J. Liu, A. C. Potter, K. T. Law, and A. Patrick Lee, “Zero-bias peaks in the tunneling conductance of spin-orbit-coupled superconducting wires with and without majorana end-states,” *Phys. Rev. Lett.* **109**, 267002 (2012).

⁶ G. Ortiz, J. Dukelsky, E. Cobanera, C. Esebbag, and C. Beenakker, “Many-body characterization of particle-conserving topological superfluids,” *Phys. Rev. Lett.* **113**, 267002 (2014).

⁷ G. Ortiz and E. Cobanera, “What is a particle-conserving topological superfluid? the fate of majorana modes beyond mean-field theory,” *Ann. Phys.* **372**, 357 (2016).

⁸ P. Bonderson, M. Freedman, and C. Nayak, “Measurement-only topological quantum computa-

tion via anyonic interferometry,” *Ann. Phys.* **324**, 787 (2009).

⁹ D. Mayers and A. Yao, “Self testing quantum apparatus,” *Quant. Inf. Comp.* **4**, 273 (2004).

¹⁰ A. Acín and *et al.*, “Device-independent security of quantum cryptography against collective attacks,” *Phys. Rev. Lett.* **98**, 230501 (2007).

¹¹ R. Colbeck and A. Kent, “Private randomness expansion with untrusted devices,” *J. Phys. A* **44**, 095305 (2011).

¹² T. Karzig *et al.*, “Scalable designs for quasiparticle-poisoning-protected topological quantum computation with majorana zero modes,” *Phys. Rev. B* **95**, 235305 (2017).

¹³ S. Popescu and D. Rohrlich, “Which states violate bell’s inequality maximally?” *Phys. Lett. A* **169**, 411 (1992).

¹⁴ E. T. Campbell, M. J. Hoban, and J. Eisert, “Majorana fermions and non-locality,” *Quant. Inf. Comp.* **14**, 0981 (2014).

¹⁵ A. Romito and Y. Gefen, “Ubiquitous nonlocal entanglement with majorana zero modes,” *Phys. Rev. Lett.* **119**, 157702 (2017).

¹⁶ A. Peres, “Incompatible results of quantum measurements,” *Phys. Rev. A* **151**, 107 (1990).

¹⁷ N. D. Mermin, “Simple unified form for the major non-hidden-variables theorems,” *Phys. Rev. Lett.* **65**, 3373 (1990).

- ¹⁸ M. McKague, “Self-testing graph states,” in *6th Conference on Theory of Quantum Computation, Communication, and Cryptography* (Springer-Verlag, New York, 2014) p. 104.
- ¹⁹ X. Wu, Y. Cai, T. H. Yang, H. N. Le, J.-D. Bancal, and V. Scarani, “Robust self-testing of the three-qubit w state,” *Phys. Rev. A* **90**, 042339 (2014).
- ²⁰ J. Kaniewski, “Analytic and nearly optimal self-testing bounds for the clauser-horne-shimony-holt and mermin inequalities,” *Phys. Rev. Lett.* **117**, 070402 (2016).
- ²¹ A. Coladangelo, K. T. Goh, and V. Scarani, “All pure bipartite entangled states can be self-tested,” *Nature Communications* **8** (2017), 10.1038/ncomms15485.
- ²² A. Kalev and C. A. Miller, “Rigidity of the magic pentagram game,” *Quantum Science and Technology* **3**, 015002 (2017).
- ²³ S. Breiner, A. Kalev, and C. A. Miller, “Parallel self-testing of the ghz state with a proof by diagrams,” in *Proceedings of the 15th International Conference on Quantum Physics and Logic, Halifax, Canada, 3-7th June 2018, Electronic Proceedings in Theoretical Computer Science, Vol. 287*, edited by Peter Selinger and Giulio Chiribella (Open Publishing Association, 2019) pp. 43–66.
- ²⁴ J. Kaniewski, “Self-testing of binary observables based on commutation,” *Phys. Rev. A* **95**, 062323 (2017).
- ²⁵ M. McKague, T. H. Yang, and V. Scarani, “Physical characterization of quantum devices from nonlocal correlations,” *J. Phys. A* **45**, 455304 (2012).
- ²⁶ M. McKague, T. H. Yang, and V. Scarani, “Robust self-testing of the singlet,” *Journal of Physics A: Mathematical and Theoretical* **45**, 455304 (2012).
- ²⁷ D. Leibfried and D. J. Wineland, “Efficient eigenvalue determination for arbitrary pauli products based on generalized spin-spin interactions,” *Journal of Modern Optics* **65**, 774–779 (2018), <https://doi.org/10.1080/09500340.2017.1423123>.
- ²⁸ A. A. Cabello, S. Filipp, H. Rauch, and Y. Hasegawa, “Proposed experiment for testing quantum contextuality with neutrons,” *Phys. Rev. Lett.* **100**, 130404 (2008).
- ²⁹ H. Bartosik *et al.*, “Experimental test of quantum contextuality in neutron interferometry,” *Phys. Rev. Lett.* **103**, 040403.
- ³⁰ T. H. Yang *et al.*, “Robust and versatile black-box certification of quantum devices,” *Phys. Rev. Lett.* **113**, 040401 (2014).
- ³¹ J.-D. Bancal *et al.*, “Physical characterization of quantum devices from nonlocal correlations,” *Phys. Rev. A* **91**, 022115 (2015).
- ³² If the state $|\Psi\rangle$ is prepared with definite outcomes $a_{r_0}^{(0)}$ of the observables A_{r_0} belonging to a context of a Peres-Mermin-like Magic square consisting of nine putative Majorana fermion parity operators, then the *ideal* probability distribution of outcomes for some row \mathcal{R}_i (column \mathcal{C}_i) is $\Pr(a_r, \dots | A_r, \dots) = \langle \Psi | \prod_r \frac{1 + a_r A_r}{2} | \Psi \rangle = \prod_r \frac{1}{2} + \omega \prod_r \frac{a_r}{2}$, where $r \in \mathcal{R}_i$ ($r \in \mathcal{C}_i$), $r_0 \in \mathcal{R}_{i_0}$, and $\omega \in \{\pm 1\}$ is determined from $\omega = \prod_{r_0} a_{r_0}^{(0)} P_{r_0} \prod_r P_r$. Using this formula one can compute the probability distribution in Table IV. For the context \mathcal{R}_1 , for example, $\omega = a_{12}^{(0)} a_{34}^{(0)} a_{56}^{(0)} P_{12} P_{34} P_{56} P_{36} P_{25} P_{14} = +1$, therefore, the probability is $1/4$, i.e., non-zero, whenever $\prod_r a_r = +1$.
- ³³ A. Peres, “Neumark’s theorem and quantum inseparability,” *Foundations of Physics* **20**, 1441–1453 (1990).
- ³⁴ S. Pironio *et al.*, “Device-independent quantum key distribution secure against collective attacks,” *New J. Phys.* **11**, 045021 (2009).

Appendix A: Ideal Expectations and Statistics

(a)

Context	$\Pr(a_r, a_s, a_t A_r, A_s, A_t)$			
	+++	+-	-+-	---
\mathcal{R}_1	0.25	0.25	0.25	0.25
\mathcal{R}_2	0.25	0.25	0.25	0.25

(b)

Context	$\Pr(a_r, a_s A_r, A_s)$			
	++	+-	-+	--
\mathcal{C}_1	0.5	0	0	0.5
\mathcal{C}_2	0.5	0	0	0.5
\mathcal{C}_3	0	0.5	0.5	0

TABLE IV. Probability Distribution of outcomes for (a) rows \mathcal{R}_i , and (b) columns \mathcal{C}_i , when the initial state is $|a_{36}^{(0)} = +1, a_{25}^{(0)} = +1, a_{14}^{(0)} = -1\rangle$. The probability of measuring (A_r, A_s, A_t) (or (A_r, A_s)) and obtaining (a_r, a_s, a_t) (or (a_r, a_s)), with $a_r, a_s, a_t \in \{-1, +1\}$, is denoted as $\Pr(a_r, a_s, a_t | A_r, A_s, A_t)$ (or $\Pr(a_r, a_s | A_r, A_s)$). Since the total parity of the (initial) state is $\mathcal{P} = +1$, it has no amplitude in states with odd total parity.

Operators in each context of Table II realize complete sets of commuting observables (CSCO), allowing preparation of states with definite parity assignments. In the following discussion, we consider the experimental preparation of an initial state with a well-defined parity $a_{36}^{(0)}$, $a_{25}^{(0)}$ and $a_{14}^{(0)}$, $a_{jk}^{(0)} \in \{-1, +1\}$, corresponding to the claimed parity observable A_{jk} . We then measure the contexts (sets of operators in a row or column) of Table III. As an illustration, the ideal probability distribution³² of measurement outcomes of all contexts for the initial state $a_{36}^{(0)} = +1, a_{25}^{(0)} = +1, a_{14}^{(0)} = -1$ is given in Table IV. From the statistics of measurement outcomes one can calculate the expectation value of the product of the operators in each context by using

$$\langle A_r A_s \rangle = \frac{\sum_{a_r, a_s} a_r a_s N(a_r, a_s)}{\sum_{a_r, a_s} N(a_r, a_s)}, \quad (\text{A1})$$

$$\langle A_r A_s A_t \rangle = \frac{\sum_{a_r, a_s, a_t} a_r a_s a_t N(a_r, a_s, a_t)}{\sum_{a_r, a_s, a_t} N(a_r, a_s, a_t)}, \quad (\text{A2})$$

where $N(a_r, a_s)$ (or $N(a_r, a_s, a_t)$) refers to the number of experimental outcomes with value (a_r, a_s) (or (a_r, a_s, a_t)). Ideal expectation values of all contexts for different initial states with all possible $a_{36}^{(0)}, a_{25}^{(0)}, a_{14}^{(0)} \in \{-1, +1\}$ is given in Table V.

Appendix B: From POVM to Projective Measurements

In this section we show, using a dilation argument, that the measurement observables in our setup can be expressed as Hermitian involutions without loss of generality. In particular, we prove Proposition 1 which states

Initial state $ a_{36}^{(0)}, a_{25}^{(0)}, a_{14}^{(0)}\rangle$	Expectation Values				
	\mathcal{R}_1	\mathcal{R}_2	\mathcal{C}_1	\mathcal{C}_2	\mathcal{C}_3
+, +, +	-1	-1	-1	-1	-1
+, +, -	+1	+1	+1	+1	-1
+, -, +	+1	+1	+1	-1	+1
+, -, -	-1	-1	-1	+1	+1
-, +, +	+1	+1	-1	+1	+1
-, +, -	-1	-1	+1	-1	+1
-, -, +	-1	-1	+1	+1	-1
-, -, -	+1	+1	-1	-1	-1

TABLE V. Expectation values of product of operators in rows (\mathcal{R}_i) and columns (\mathcal{C}_i) for different initial states.

that projectors obtained by dilation have the same pairwise commutativity structure as those assumed for the elements of the corresponding POVMs.

Given any POVM $\{Q_a\}$, $a = 0, 1, \dots, d-1$, acting on system \mathcal{S} , Neumark proved³³ that there exists a projective measurement $\{\hat{Q}_a\}$ on an extended system $\mathcal{S} \otimes \mathcal{E}$, with $\text{Tr}(\hat{Q}_a(\rho \otimes |0\rangle\langle 0|_{\mathcal{E}})) = \text{Tr}(Q_a \rho)$ for all density operators ρ on \mathcal{S} , where the dimension of the extension \mathcal{E} equals the number of elements d in the POVM. The projectors are of the form

$$\hat{Q}_a = U_{\mathcal{S}\mathcal{E}}^\dagger (\mathbb{1}_{\mathcal{S}} \otimes |a\rangle\langle a|_{\mathcal{E}}) U_{\mathcal{S}\mathcal{E}}, \quad (\text{B1})$$

where $U_{\mathcal{S}\mathcal{E}}$ is a unitary on the extended Hilbert space. In our case, we further require that the projectors obtained by dilation have the same pairwise commutativity structure that was assumed of the two-element POVMs which we prove in the following proposition.

Proposition 1. *Let $\{Q_{r,a}\}$ be a set of two-outcome POVM elements. Then there exist projectors $\hat{Q}_{r,a}$ satisfying $\text{Tr}(\hat{Q}_{r,a}(\rho \otimes |0\rangle\langle 0|_r)) = \text{Tr}(Q_{r,a}\rho)$ for all density operators ρ , and $[\hat{Q}_{r,a}, \hat{Q}_{s,b}] = 0$ whenever $[Q_{r,a}, Q_{s,b}] = 0$.*

Proof. Define the projector $\hat{Q}_{r,a}$ on the extended system $\mathcal{S} \otimes \mathcal{E}_r$ corresponding to POVM element $Q_{r,a}$ according to Eq. (B1), with

$$U_{\mathcal{S}\mathcal{E}_r} |\Psi\rangle \otimes |a\rangle_r = \sum_{b=0}^1 (-1)^{ab} \sqrt{Q_{r,a\oplus b}} |\Psi\rangle \otimes |b\rangle_r,$$

where $|a\rangle_r$ is the basis-vector of the extension \mathcal{E}_r with $a \in \{0, 1\}$ and \oplus denotes addition mod 2. We first show that $U_{\mathcal{S}\mathcal{E}_r}$ is unitary. Indeed, we have

$$\begin{aligned} & \langle \Phi | \langle a | U_{\mathcal{S}\mathcal{E}_r}^\dagger U_{\mathcal{S}\mathcal{E}_r} | \Psi \rangle | b \rangle_r \\ &= \sum_{c=0}^1 (-1)^{(a+b)c} \langle \Phi | \sqrt{Q_{r,a\oplus c}} \sqrt{Q_{r,b\oplus c}} | \Psi \rangle. \end{aligned}$$

If $a = b$, then the last line above equals

$$\langle \Phi | \sum_{c=0}^1 Q_{r,c} | \Psi \rangle = \langle \Phi | \Psi \rangle,$$

whereas if $a \neq b$, it equals

$$\langle \Phi | (\sqrt{Q_{r,a}}\sqrt{Q_{r,b}} - \sqrt{Q_{r,b}}\sqrt{Q_{r,a}}) | \Psi \rangle = 0,$$

where we've used $Q_{r,b} = \mathbb{1}_S - Q_{r,a}$ and thus $\sqrt{Q_{r,a}}$ commutes with $\sqrt{Q_{r,b}}$. Therefore, $U_{S\mathcal{E}_r}$ is unitary. Next, using the cyclic property of the trace, we compute

$$\begin{aligned} & \text{Tr}(\hat{Q}_{r,a}(\rho \otimes |0\rangle\langle 0|_r)) \\ &= \text{Tr}(U_{S\mathcal{E}_r}(\rho \otimes |0\rangle\langle 0|_r)U_{S\mathcal{E}_r}^\dagger(\mathbb{1}_S \otimes |a\rangle\langle a|_r)) \\ &= \text{Tr}(\sqrt{Q_{r,a}}\rho\sqrt{Q_{r,a}}) \\ &= \text{Tr}(Q_{r,a}\rho). \end{aligned}$$

Finally, for $s \neq r$, in a block matrix representation with respect to the $|a\rangle_r$ basis,

$$U_{S\mathcal{E}_r} = \begin{pmatrix} \sqrt{Q_{r,0}} & \sqrt{Q_{r,1}} \\ \sqrt{Q_{r,1}} & -\sqrt{Q_{r,0}} \end{pmatrix}, \quad \hat{Q}_{s,b} = \begin{pmatrix} Q_{s,b} & 0 \\ 0 & Q_{s,b} \end{pmatrix}.$$

Therefore, $[Q_{r,a}, Q_{s,b}] = 0$ implies that $[U_{S\mathcal{E}_r}, \hat{Q}_{s,b}] = 0$, and hence $[\hat{Q}_{r,a}, \hat{Q}_{s,b}] = 0$. \square

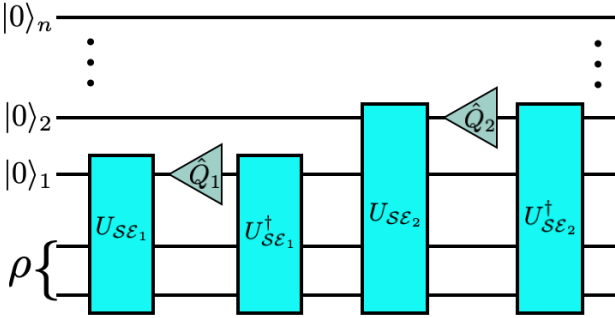


FIG. 3. Dilation extension in quantum circuit language.

In the case of multiple POVMs Q_r , where r labels the POVM with elements $\{Q_{r,a}\}$, the POVMs can be extended to projectors $\{\hat{Q}_{r,a}\}$ by adding several ancillas $(\otimes_r \mathcal{E}_r)$, one for each POVM. The situation is depicted in Fig. 3.

Having extended the POVMs to projective measurements, we can define the Hermitian operators $A_r = 2\hat{Q}_{r,0} - \mathbb{1}$. Note that $A_r^2 = \mathbb{1}$, and so each A_r is unitary and has eigenvalues in $\{-1, +1\}$.

Appendix C: Jordan's Lemma

We prove a corollary, which we used in the main text, of what is known as Jordan's Lemma in the quantum information literature. A particularly simple proof of Jordan's Lemma appears in Ref. [34], which we also include here for completeness.

Lemma 7 (Jordan's Lemma). *Let A_1 and A_2 be Hermitian involutions on a Hilbert space \mathcal{H} . Then \mathcal{H} decomposes as a direct sum $\mathcal{H} = \bigoplus_l \mathcal{H}_l$, with $\dim \mathcal{H}_l \in \{1, 2\}$, and A_1 and A_2 act invariantly on each \mathcal{H}_l .*

Proof. $A_1 A_2$ is unitary since $(A_1 A_2)(A_1 A_2)^\dagger = A_1 A_2 A_2 A_1 = \mathbb{1}$. Since $A_1 A_2$ is unitary, there exists an orthonormal basis for \mathcal{H} of eigenstates of $A_1 A_2$. Let $|\alpha\rangle$ be any such eigenstate, where $A_1 A_2 |\alpha\rangle = \alpha |\alpha\rangle$. Define $|\bar{\alpha}\rangle = A_1 |\alpha\rangle$. Then $A_1 A_2 |\bar{\alpha}\rangle = \bar{\alpha} |\bar{\alpha}\rangle$, since

$$A_1 A_2 A_1 |\alpha\rangle = A_1 (A_1 A_2)^\dagger |\alpha\rangle = \bar{\alpha} A_1 |\alpha\rangle.$$

The span of $|\alpha\rangle$ and $|\bar{\alpha}\rangle$ is invariant under A_1 , and also under A_2 , since

$$A_2 |\alpha\rangle = A_2 A_1 |\bar{\alpha}\rangle = (A_1 A_2)^\dagger |\bar{\alpha}\rangle = \alpha |\bar{\alpha}\rangle,$$

$$A_2 |\bar{\alpha}\rangle = A_2 A_1 |\alpha\rangle = (A_1 A_2)^\dagger |\alpha\rangle = \bar{\alpha} |\alpha\rangle.$$

Thus any eigenstate of $A_1 A_2$ defines an invariant subspace of dimension at most 2, and these eigenstates span \mathcal{H} , which completes the proof. \square

Corollary 7.1. *For $k, k' \in \{1, 2\}$, let A_k and $B_{k'}$ be Hermitian involutions with $[A_k, B_{k'}] = 0$. Then \mathcal{H} decomposes as $\mathcal{H} = \bigoplus_l (\mathcal{H}_{a_l} \otimes \mathcal{H}_{b_l})$, with \mathcal{H}_{a_l} and \mathcal{H}_{b_l} of dimension at most 2, and $A_k = \bigoplus_l (A_{k_l} \otimes \mathbb{1}_l)$ and $B_{k'} = \bigoplus_l (\mathbb{1}_l \otimes B_{k'_l})$.*

Proof. Note that $[A_1 A_2, B_1 B_2] = 0$. Thus, there exists an orthonormal basis for \mathcal{H} of simultaneous eigenstates of $A_1 A_2$ and $B_1 B_2$. Let $|\alpha, \beta\rangle$ be any such eigenstate, where $A_1 A_2 |\alpha, \beta\rangle = \alpha |\alpha, \beta\rangle$ and $B_1 B_2 |\alpha, \beta\rangle = \beta |\alpha, \beta\rangle$. Define $|\bar{\alpha}, \beta\rangle = A_1 |\alpha, \beta\rangle$, $|\alpha, \bar{\beta}\rangle = B_1 |\alpha, \beta\rangle$, and $|\bar{\alpha}, \bar{\beta}\rangle = A_1 B_1 |\alpha, \beta\rangle$. Then $\text{span}\{|\alpha, \beta\rangle, |\bar{\alpha}, \beta\rangle, |\alpha, \bar{\beta}\rangle, |\bar{\alpha}, \bar{\beta}\rangle\}$ maps isomorphically to $\text{span}\{|\alpha\rangle, |\bar{\alpha}\rangle\} \otimes \text{span}\{|\beta\rangle, |\bar{\beta}\rangle\}$. By the argument in the proof of Lemma 7, A_k and $B_{k'}$ act invariantly on the first and second tensor factors, and trivially on the second and first tensor factors, respectively. \square

We remark that in the main text we assume that each Jordan subspace \mathcal{H}_l has dimension 4. This is done without loss of generality, since we can extend any smaller dimensional subspace to 4 dimensions, with all operators acting trivially on the extension.

Appendix D: Derivation of Eqs. (9) and (10).

It will be convenient to work in the Y basis $\{|0_Y 0_Y\rangle, |0_Y 1_Y\rangle, |1_Y 0_Y\rangle, |1_Y 1_Y\rangle\}$ within each Jordan subspace \mathcal{H}_l . Here $|0_Y\rangle = (|0\rangle + i|1\rangle)/\sqrt{2}$, and $|1_Y\rangle = (|0\rangle - i|1\rangle)/\sqrt{2}$. We expand $|\Psi_l\rangle$ as

$$|\Psi_l\rangle = \sum_{a,b \in \{0,1\}} c_{ab}^l |a_Y b_Y\rangle,$$

where $\sum_{a,b} |c_{ab}^l|^2 = 1$. In this basis, the ideal state is

$$|\hat{\Psi}\rangle = \sum_l \sqrt{\frac{p_l}{2}} (|0_Y 1_Y\rangle + |1_Y 0_Y\rangle)$$

Our first step is to bound $\sum_l p_l (|c_{00}^l|^2 + |c_{11}^l|^2)$. Applying Eq. (5) to \mathcal{C}_1 and \mathcal{C}_2 , respectively, we obtain

$$\sum_l p_l (|c_{00}^l - c_{11}^l|^2 + |c_{01}^l - c_{10}^l|^2) \leq \epsilon,$$

$$\sum_l p_l (|e^{-i\phi_l} c_{00}^l + e^{i\theta_l} c_{11}^l|^2 + |e^{i\phi_l} c_{01}^l - e^{i\theta_l} c_{10}^l|^2) \leq \epsilon,$$

Eq. (10) follows from the first of these equations. It also follows that

$$\sum_l p_l |c_{00}^l - c_{11}^l|^2 \leq \epsilon. \quad (\text{D1})$$

$$\sum_l p_l |e^{-i\phi_l} c_{00}^l - e^{i\theta_l} c_{11}^l|^2 \leq \epsilon. \quad (\text{D2})$$

Now,

$$\begin{aligned} & |c_{11}^l|^2 |e^{i\theta_l} + e^{-i\phi_l}|^2 \\ &= |(e^{i\theta_l} c_{11}^l + e^{-i\phi_l} c_{00}^l) - e^{-i\phi_l} (c_{00}^l - c_{11}^l)|^2 \\ &\leq 2(|e^{i\theta_l} c_{11}^l + e^{-i\phi_l} c_{00}^l|^2 + |c_{00}^l - c_{11}^l|^2), \end{aligned}$$

where in the last line we used the fact that $|x + y|^2 \leq 2(|x|^2 + |y|^2)$ for any $x, y \in \mathbb{C}$. From Eqs. (D1) and (D2),

$$\begin{aligned} & \sum_l p_l |c_{11}^l|^2 |e^{i\theta_l} + e^{-i\phi_l}|^2 \\ &= \sum_l p_l |c_{11}^l|^2 (2 + 2 \cos(\theta_l + \phi_l)) \leq 4\epsilon \quad (\text{D3}) \end{aligned}$$

Similarly,

$$\begin{aligned} & |c_{00}^l|^2 |e^{i\theta_l} + e^{-i\phi_l}|^2 \\ &= |(e^{i\theta_l} c_{11}^l + e^{-i\phi_l} c_{00}^l) + e^{i\theta_l} (c_{00}^l - c_{11}^l)|^2 \\ &\leq 2(|e^{i\theta_l} c_{11}^l + e^{-i\phi_l} c_{00}^l|^2 + |c_{00}^l - c_{11}^l|^2), \end{aligned}$$

from which it follows that

$$\begin{aligned} & \sum_l p_l |c_{00}^l|^2 |e^{i\theta_l} + e^{-i\phi_l}|^2 \\ &= \sum_l p_l |c_{00}^l|^2 (2 + 2 \cos(\theta_l + \phi_l)) \leq 4\epsilon. \quad (\text{D4}) \end{aligned}$$

Adding Eqs. (D3) and (D4),

$$\sum_l p_l (|c_{00}^l|^2 + |c_{11}^l|^2) (1 + \cos(\theta_l + \phi_l)) \leq 4\epsilon. \quad (\text{D5})$$

We now need the following Lemma, which is similar to Lemma 6.

Lemma 8. *Suppose the ideal expectations are satisfied to within error ϵ . Then $\|A_{12}A_{34}|\Psi\rangle + A_{16}A_{45}|\Psi\rangle\| \leq 3\sqrt{2}\epsilon$.*

Proof.

$$\begin{aligned} & \|A_{12}A_{34}|\Psi\rangle + A_{16}A_{45}|\Psi\rangle\| \\ &\leq \|(A_{12}A_{34} - A_{56})|\Psi\rangle\| + \|(A_{56} + A_{23})|\Psi\rangle\| \\ &\quad + \|(-A_{23} + A_{16}A_{45})|\Psi\rangle\| \\ &\leq 3\sqrt{2}\epsilon \end{aligned}$$

where the last inequality follows from Eqs. (5) and (6). \square

From the result of the Lemma, we obtain

$$\begin{aligned} & \sum_l p_l (|c_{00}^l|^2 + |c_{11}^l|^2) |e^{i\theta_l} + e^{i\phi_l}|^2 \\ &\quad + (|c_{01}^l|^2 + |c_{10}^l|^2) |e^{i\theta_l} - e^{-i\phi_l}|^2 \leq 18\epsilon, \end{aligned}$$

and therefore,

$$\sum_l p_l (|c_{00}^l|^2 + |c_{11}^l|^2) |e^{i\theta_l} + e^{i\phi_l}|^2 \leq 18\epsilon,$$

or,

$$\sum_l p_l (|c_{00}^l|^2 + |c_{11}^l|^2) (1 + \cos(\theta_l - \phi_l)) \leq 9\epsilon. \quad (\text{D6})$$

Adding Eqs. (D5) and (D6),

$$\begin{aligned} \frac{13}{2}\epsilon &\geq \sum_l p_l (|c_{00}^l|^2 + |c_{11}^l|^2) (1 + \cos \theta_l \cos \phi_l) \\ &\geq \sum_l p_l (|c_{00}^l|^2 + |c_{11}^l|^2). \end{aligned}$$

where in the last inequality we used $\theta_l, \phi_l \in [-\frac{\pi}{2}, \frac{\pi}{2}]$, and so $\cos \theta_l \geq 0$ and $\cos \phi_l \geq 0$. This last inequality is Eq. (9) in the main text.

Appendix E: Derivation of Eq. (15)

By definition,

$$\langle \hat{\Psi}_l | (\mathbf{1} - \hat{A}_{34} A_{34}) | \Psi_l \rangle = \frac{(c_{01}^l + c_{10}^l) - (c_{01}^l e^{i\phi_l} + c_{10}^l e^{-i\phi_l})}{\sqrt{2}}.$$

Therefore,

$$\begin{aligned} & \text{Re} \langle \hat{\Psi}_l | (\mathbf{1} - \hat{A}_{34} A_{34}) | \Psi_l \rangle \\ &= \frac{(1 - \cos \phi_l) \text{Re}(c_{01}^l + c_{10}^l) + \sin \phi_l \text{Im}(c_{01}^l - c_{10}^l)}{\sqrt{2}} \\ &\leq (1 - \cos \phi_l) + \frac{\sin \phi_l \text{Im}(c_{01}^l - c_{10}^l)}{\sqrt{2}}. \end{aligned}$$

Summing over the Jordan subspaces, we get

$$\begin{aligned}
& \sum_l p_l \operatorname{Re} \langle \hat{\Psi}_l | (\mathbf{1} - \hat{A}_{34} A_{34}) | \Psi_l \rangle \\
& \leq 1 - \sum_l p_l \cos \phi_l + \frac{1}{\sqrt{2}} \sum_l p_l \sin \phi_l \operatorname{Im}(c_{01}^l - c_{10}^l) \\
& \leq 1 - \sum_l p_l \cos^2 \phi_l + \frac{1}{\sqrt{2}} \sum_l p_l \sin \phi_l |c_{01}^l - c_{10}^l| \\
& = \sum_l p_l \sin^2 \phi_l + \frac{1}{\sqrt{2}} \sum_l p_l \sin \phi_l |c_{01}^l - c_{10}^l|. \quad (\text{E1})
\end{aligned}$$

The second term in the last line is bounded by

$$\begin{aligned}
\sum_l p_l \sin \phi_l |c_{01}^l - c_{10}^l| & \leq \sqrt{\sum_l p_l \sin^2 \phi_l} \sqrt{\sum_l p_l |c_{01}^l - c_{10}^l|^2} \\
& \leq \sqrt{\frac{25\epsilon}{2}} \sqrt{\epsilon},
\end{aligned}$$

where we've used Eq. (10) and the same argument leading to Eq. (12), applied to ϕ_l . Therefore,

$$\begin{aligned}
\sum_l p_l \operatorname{Re} \langle \hat{\Psi}_l | (\mathbf{1} - \hat{A}_{34} A_{34}) | \Psi_l \rangle & \leq \frac{25}{2} \epsilon + \frac{1}{\sqrt{2}} \frac{5\epsilon}{\sqrt{2}} \\
& = 15\epsilon.
\end{aligned}$$

Using this bound we can say

$$\begin{aligned}
\operatorname{Re} \langle \hat{\Psi} | \hat{A}_{34} A_{34} | \Psi \rangle & \geq \operatorname{Re} \langle \hat{\Psi} | \Psi \rangle - |\operatorname{Re} \langle \hat{\Psi} | (\mathbf{1} - \hat{A}_{34} A_{34}) | \Psi \rangle| \\
& \geq 1 - 7\epsilon - 15\epsilon \\
& = 1 - 22\epsilon.
\end{aligned}$$

Therefore,

$$\begin{aligned}
\|A_{34} |\Psi\rangle - \hat{A}_{34} |\hat{\Psi}\rangle\| & = \sqrt{2 - 2 \operatorname{Re} \langle \hat{\Psi} | \Psi \rangle} \\
& \leq \sqrt{44\epsilon}.
\end{aligned}$$